DOI: https://doi.org/10.57233/ijsgs.v10i1.600 ISSNp: 2488-9229; ISSNe: 3027-1118

IJSGS FUGUSAU VOL. 10(1) WEBSITE: https://fugus-ijsgs.com.ng

INTERNATIONAL JOURNAL OF SCIENCE FOR GLOBAL SUSTAINABILITY

(A PUBLICATION OF FACULTY OF SCIENCE, FEDERAL UNIVERSITY GUSAU, NIGERIA)

Free Convective MHD Flow of Jeffrey Fluid in a Porous Medium in the Presence of Heat Source/Sink

Aisha Umar Dakin-Gari *[1], N. M. Sarki[2], M. M. Hamza[4], S. M. Dakin-Gari[5] and I. D. Yale.[2,3]

[1]Department of Mathematics, Federal University Birnin-Kebbi, Nigeria.

[2]Department of Mathematics, Kebbi State University of Science and Technology, Aliero.

[3]Department of Electrical, Telecommunication and Computer Engineering, Kampala International University, Western Campus, Uganda.

[4] Department of Mathematics, Usmanu Danfodio University Sokoto.

[5] Department of Mathematics, Kebbi State Polytechnic, Dakingari.

***Corresponding Author's Email:** aishaumardkg@gmail.com

Received on: January, 2024 **Revised and Accepted on:** March 2024 **Published on:** March 2024

ABSTRACT

The heat and mass transfer being a driving force in MHD oscillatory free convective flow has been a subject of many studies due to the increasing demand associated with transport processes, existing in nature and industrial application. This study is carried out to investigate an effect of heat and mass transfer on unsteady MHD free convective flow of Jeffrey fluid through porous medium in the presence of heat source. The dimensional governing equations were solved by perturbation technique. The solution for the flow characteristics of velocity, temperature and concentration was obtained. The influence of different parameters such as: thermal Grashof number, mass Grashof number, Jeffrey parameter and heat source/sink, Peclet number for heat and mass transfer (Pe & Pem), and radiation parameter were investigated on the flow fields and presented graphically. The fluid velocity decreases with increase in Hartmann number (H). It is found that mass transfer rate increases with increase in Peclet number(Pem). It is noticed that rate of mass diffusion decreases with increase in chemical reaction parameter (K). In addition, the temperature profiles depicted that an increase as the values of heat source/sink parameter(Q), heat transfer Peclet number (Pe), and radiation parameter (N) increases respectively.

Keywords: Jeffery fluid, Unsteady free convection, Porous medium, Magnetohydrodynamics (MHD) and Heat source/sink

1.0 INTRODUCTION

Fluids can majorly be categorized into two classes; Newtonian and non-Newtonian fluids. Newtonian fluids are those fluids that obey Newton's law of viscosity. Those fluids that deviate from the law are said to be non-Newtonian. Typical non-Newtonian fluids include blood, saliva, starch solutions, toothpaste, and sauces. Due to the fact that non-Newtonian fluids cannot be described by a single constitutive equation like the Navier–Stokes equations, they tend to be more complicated than Newtonian fluids. Although complicated, non-Newtonian fluids have found more industrial applications than Newtonian fluids. Recently, there is much attention which has been paid on the study of non-Newtonian fluid flow. The non-Newtonian fluids can be characterised as being of the differential, rate or integral type, (Cioranescu *et al.* 2016). Some of the non-Newtonian models which have been studied include the Jeffrey model (Nadeem *et al.* 2021), the Maxwell model (Sajid *et al.* 2021), the Oldroyd-B model (Wang *et al.* 2019), and the Herschel–Bulkley model (Magnon and Cayeux 2021). One non-Newtonian fluid model of interest in this study is the Jeffrey model which is of the rate type. The Jeffrey fluid expresses the influence of the ratio of relaxation to retardation times and its constitutive equation can be reduced to that of a Newtonian fluid as a special case. Unlike viscous fluid models, the Jeffrey model can be used in non-Newtonian fluids to describe the stress relaxation property (Kahshan *et al.* 2019). Due to its viscoelastic properties, the Jeffrey fluid has found some industrial applications in polymer productions. The Jeffrey fluid model has recently attracted the attention of many researchers since it gives better approximations to most physiological fluids. To this end, Suma et al. (2023) recently discussed the implication of Brownian motion and thermophoresis impacts on a hydromagnetic heat and mass transfer with Jeffrey fluid flow affected by nanoparticle along an upstanding plate. Yale *et al.* (2019) studied transient heat transfer to MHD oscillatory flow of Jeffry fluid through a porous medium under slip condition and oscillating temperature. In another article, the effect suction/injection on MHD oscillatory flow of Jeffry fluid with heat source/sink through a porous medium was investigated by Ibrahim *et al.* (2020). Additionally, Sharma *et al.* (2017) used the Jeffrey fluid to model the flow of blood in narrow arteries. Some other researches which have been completed on the Jeffrey model include the works by Khan *et al.* (2018) and Vaidya *et al.* (2020).

Magneto-hydrodynamics (MHD) is the study of electrically conducting liquids, such as salty water, electrolytes, plasma, and liquid metals. This type of fluid has a number of engineering and industrial applications such as in growth of crystals, reactor cooling, magnetic drug targeting, MHD sensors, and power generation. MHD is dependent on the intensity

of magnetic induction (Jawad *et al*. 2021). The experimental investigation of modern MHD flow in a laboratory was first carried out by Hartmann and Lazarus (1937). This study provided the basic knowledge for the development of many MHD devices, such as MHD pumps, MHD generators, brakes, flow meters, plasma studies, and geothermal energy extraction. Since then, many works have been carried out to investigate the impacts of MHD on free convection flow through various channels. Free convection flows through an oscillatory flow in the involvement of heat source through a porous medium has been a subject of growing interest of many researchers due to its wide spectrum of applications in geophysics, solid mechanics, ground water, hydrology, oil recovery, thermal insulation, heat storage and in the field of engineering (Chitra and Suhasini, 2018). In view of the many applications of MHD oscillatory heat transfer flows, Usman and Sanusi (2023) recently explored the effects of non-Newtonian nanofluid flows across a semi-infinite flat plate immersed in a porous medium on heat radiation, Soret and pressure terms. They took into account the surface temperature and concentration, which are oscillatory in nature due to the presence of various types of nanoparticles. Bafakeeh *et al*. (2022) discussed the unsteady hydromagnetic oscillatory natural convective heat and mass transfer flow of a viscous and electrically conducting fluid passing through a vertical plate immersed in a permeable medium in the coexistence of chemical reactions and thermal radiation affected by Hall current and Soret factor. Narayana and Venkateswarlu (2016) studied the consequences of chemical reaction and heat source effects on unsteady MHD free convection heat and mass transfer of a nanofluid flow past a semi-infinite flat plate in a rotating system. The plate is assumed to oscillate in time with steady frequency so that the solutions of the boundary layer are the similar oscillatory type. Sharma *et al.* (2022) emphasized the analytical study of MHD oscillatory time-dependent free convective viscous incompressible dissipative flow passing through an upstanding channel entrenched with porous medium in the coexistence of heat generation and thermal radiation factors. Falade *et al.* (2017) investigated the implications of suction/injection effects on a time-dependent oscillatory slip flow within an upright vertical channel with unequal wall heating restricted to a transverse magnetic field. Hamza *et al*. (2011) researched the impacts of chemical reaction and slip condition on a time-dependent hydromagnetic heat and mass transfer flow across an upstanding channel saturated with porous medium in a rotating system.

Investigating the effect of heat generation or absorption on fluid flow is extremely fundamental in several technological and physical problems of exothermic or endothermic fluid response nowadays, and these effects are crucial in monitoring the heat transference (Gambo *et al*. 2021). Several scholars have investigated the effects of heat-generating/absorbing fluid on various flow regimes. In this context, Ojemeri *et al.* (2024) recently published an analytical investigation of a chemically reactive hydromagnetic fluid affected by heat generation/absorption flowing across a superhydrophobic microchannel that is heated alternatively. In addition, Ojemeri and Onwubuya (2023) described the analysis of steady mixed convection flow of Arrhenius-controlled chemical reaction and an exothermic fluid along an isothermally heated superhydrophobic microchannel due to heat source/sink. In another paper, Ojemeri and Hamza (2022) presented a theoretical investigation of a chemically reactive fluid in a MHD natural convection flow blended with heat source and sink effects employing homotopy perturbation approach. They concluded that raising the viscous heating parameter significantly encourage the fluid motion and the volume flow rate respectively. Oni and Jha (2019) investigated the effects of a heat source and sink fluid on natural convection confined to an upstanding annulus with time-periodic heating boundary conditions. They discovered that heat generation and absorption parameters affect velocity distribution, periodic temperature profile, Nusselt number, and frictional force at the cylinder walls, respectively. Gambo and Gambo (2020) extensively scrutinized the effects of fully developed natural convective flow of heat generating/absorbing fluid in an open-ended vertical concentric annulus with a magnetic field effect. Their findings show that by carefully selecting appropriate values for the heat generation or absorption parameter and the Hartmann number, they may be used to control the temperature and velocity profiles. Chu *et al*. (2020) investigated the nonlinear thermal radiation and heat sink/source of a bidirectional periodically moving surface driven flow in a rate type nanofluid containing a gyrotactic microbe. Zhao *et al*. (2021) highlighted the effects of heat generation/absorption, dissipation, radiative heat flux and joule heating on the mixed convective entropy optimized nanomaterial MHD flow of Ree-Eyring fluid formed by two rotating disks. The consequences of thermal radiation, a heat source, and an induced magnetic field on the natural convective flow of a couple stress fluid in a flux-isothermal vertical channel have been evaluated by Hasan *et al*. (2020) using the method of an indeterminate coefficient. Parthiban and Pasad (2023) outlined a theoretical investigation of radiative-convection effects on MHD fluid flow in a heated square enclosure having a non-Darcy square cavity in the coexistence of the Hall effect and the heat source or sink.

The ultimate objective of the present analysis is to study Unsteady MHD free convective flow of Jeffrey fluid through porous medium with effect of heat source/sink. Equations of momentum, energy and

DOI: https://doi.org/10.57233/ijsgs.v10i1.600 ISSNp: 2488-9229; ISSNe: 3027-1118
IJSGS FUGUSAU VOL. 10(1) WEBSITE: https://fugus-ijsgs.com.ng

diffusion, which govern the fluid flow, heat and mass transfer are solved by using perturbation technique. The effects of various physical parameters on fluid velocity, temperature, concentration, skin friction coefficient, Nusselt number and Sherwood number at the plates are derived, discussed and shown through graphs.

2.0 MATHEMATICAL FORMULATION

Consider an oscillatory flow of Jeffrey fluid and heat transfer through a porous medium in a vertical infinite channel with effect of heat source/sink in the presence of transverse magnetic field. The radiative heat term in horizontal direction is considered negligible in comparison with vertical direction. At time t' □□□□, the plate is given an impulsive motion in a horizontal direction with uniform mean velocity U. The x'- axis is taken along the plate (when y □□0) and a straight line perpendicular to that as the y' -axis. A magnetic field of uniform strength B_0 is applied normal to the plate along x' -direction and the induced magnetic field is assumed negligible. It is assumed that the flow is subjected to suction of the fluid from one porous plate and at the same rate fluid is being injected through the other porous plate. It is also assumed that the fluid has small electrical conductivity and the electromagnetic force produced is very small. The pressure gradient is also assumed negligible. Since the plate is considered infinite in x' -direction, all the physical variables will be independent of x' and are functions of y' and t'. Under the usual Boussinesq's approximation, the governing equations of momentum, energy and Concentration are written as follows:

Momentum equation

$$\frac{\partial u\prime}{\partial t\prime}-v\frac{\partial u'}{\partial y'}=-\frac{1}{\rho}\frac{\partial p'}{\partial x'}+\frac{v}{(1+\beta_1)}\ \frac{\partial^2 u'}{\partial y'^2}-\frac{v}{k'}u'-\frac{\sigma_e B_0^2 u'}{\rho}+g\beta(T'-T'_0)+g\beta(C'-C'_0) \quad (1)$$

Energy equation

$$\frac{\partial T'}{\partial t'}-v\frac{\partial u'}{\partial y'}=\frac{k}{\rho c_p}\frac{\partial^2 T'}{\partial y'^2}-\frac{1}{\rho c_p}\frac{\partial q'}{\partial y'}\pm\frac{Q'}{\rho c_p}(T'-T'_0)-\frac{\sigma_e B_0^2 u'}{\rho}\ (T'-T'_0) \quad (2)$$

Concentration equation

$$\frac{\partial c'}{\partial t'}-v'\frac{\partial c'}{\partial y'}=D'\frac{\partial' C'}{\partial y'^2} \quad (3)$$

With the initial and boundary condition

$$u'-\gamma^*\frac{\partial u'}{\partial y'}=0, T'=T_0, C'=C_0' \text{on } y'=0$$
$$u'=0, T'=T_0'+\left(T_\omega'-T_0'\right)\cos\omega' t', C'=C_0'+\left(C_\omega'+C_0'\right)\cos\omega' t' \text{on } y'=a \quad (4)$$

where u' is the axial velocity, t' is time, ω' is frequency of the oscillation, T' the fluid temperature, p is the pressure gravitational force, $c_p$is the specific heat at constant pressure, k is the thermal conductivity, q is the radiative heat flux, β is the coefficient of volume expansion, k' is the porous medium permeability coefficient, B_0 is the electromagnetic induction, $\sigma_e$is the conductivity of the fluid, ρ is the denity of the fluid, v is the kinematics viscosity coefficient. It is assumed that walls temperature, T_0', T_ω' are high enough to induce radiative heat transfer, and γ^* is the dimensionless slip parameter. Following Makinde and Mhone (2005), it is assumed that the fluid is optically thin with a relatively low density and the radiative heat flux is given by:

$$\frac{\partial q\prime}{\partial y\prime}=4\alpha^2(T'_0-T') \quad (5)$$

where α is the mean radiation absorption coefficient.

To solve equations (1) – (3), we employ the dimensionless quantities and parameters:

$$\left.\begin{aligned} x=\frac{x'}{a}\Rightarrow x'=xa, y=\frac{y'}{a}\Rightarrow y'=ya, V_0=\frac{v'}{U}\Rightarrow v'=V_0U, u=\frac{u'}{U}\Rightarrow u'=uU,\\ w=\frac{w'a}{U}\Rightarrow w'=\frac{wU}{a}, t=\frac{t'U}{a}\Rightarrow t'=\frac{ta}{U}, \theta=\frac{T'-T'_0}{T'_\omega-T'_0}\Rightarrow T'=T'_0+\theta(T'_\omega-T'_0),\\ p=\frac{ap'}{\rho vU}\Rightarrow p'=\frac{p\rho vU}{a},\ \gamma=\frac{\gamma^*}{a}\Rightarrow\gamma^*=\gamma a, S^S=\frac{1}{Da}, Da=\frac{K'}{a^2}\Rightarrow k'=a^2Da\\ N^2=\frac{4\alpha^2a^2}{k}, H^2=\frac{a^2\sigma_eB_0^2}{\rho v}, Gr=\frac{g\beta(T'_\omega-T'_0)a^2}{vU}, Pe=\frac{Ua\rho c_p}{k}, Re=\frac{Ua}{v}, Q=\frac{Q'a^2}{k}\\ \phi=\frac{C'-C'_0}{C'_\omega-C'_0}\Rightarrow C'=C'_0+\phi\ (C'_\omega-C'_0), Gc=\frac{g\beta(C'_\omega-C'_0)a^2}{vU} \end{aligned}\right\} \quad (6)$$

Incorporating equation (6) in equation (1), (2), and (3), the governing equations now become:

$$Re[\frac{\partial u}{\partial t}-V_0\frac{\partial u}{\partial y}]=-\frac{\partial P}{\partial x}+\ \frac{1}{(1+\beta_1)}\frac{\partial^2 u}{\partial y^2}-(H^2+S^2)u+\mathrm{Gr}\theta+Gc\phi \quad \textbf{(7)}$$

DOI: https://doi.org/10.57233/ijsgs.v10i1.600 ISSNp: 2488-9229; ISSNe: 3027-1118
IJSGS FUGUSAU VOL. 10(1) WEBSITE: https://fugus-ijsgs.com.ng

$$Pe\left[\frac{\partial\theta}{\partial t} - V_0\frac{\partial\theta}{\partial y}\right] = \frac{\partial^2\theta}{\partial y^2} + (N^2 \pm Q - H^2)\theta \quad (8)$$

$$Pe_m\left[\frac{\partial\emptyset}{\partial t} - Vo\frac{\partial\emptyset}{\partial y}\right] = \frac{\partial^2\emptyset}{\partial y^2} \quad (9)$$

where u is dimensionless velocity, t the dimensionless time, y dimensionless coordinate axis normal to the plates, θ dimensionless temperature, $\emptyset$ dimensionless concentration, Re the Reynolds number, *Ha* Hartmann number, *Gr* Grashof number, *Gc* modified Grashof number, *Pe* Peclet number, *N* Radiation parameter, *Q* heat source/sink parameter, Pe_m Peclet number for mass transfer, Vo sunction/injection parameter and *Sc* Schmidt number.
The initial and boundary conditions in dimensionless form are given by:

$$\left.\begin{array}{l} u - \gamma\frac{\partial u}{\partial y} = 0, \theta = 0, \phi = 0 \; at \; y = 0 \\ u = 0, \theta = cos\,\omega t, \phi = cos\omega t at \; y = 1 \end{array}\right\} \quad (10)$$

3.0 METHOD OF SOLUTION

The dimensionless governing equations (6), (7) and equation (8) subject to boundary conditions (10) are solved by regular perturbation techniques.
Solving the equations for purely oscillatory flow, let the pressure gradient, fluid velocity, temperature and concentration be:

$$u = u_o e^{i\omega t} + u_1 e^{-i\omega t} \quad (11)$$

$$\theta = \theta_o e^{i\omega t} + \theta_1 e^{-i\omega t} \quad (12)$$

$$\phi = \phi_o e^{i\omega t} + \phi_1 e^{-i\omega t} \quad (13)$$

$$It \; is \; assume \; that \; -\frac{\partial p}{\partial x} = \curlywedge\,[e^{i\omega t} + e^{-i\omega t}]$$

Substituting (11), (12) and (13) into (7), (8) and (9) the solutions of the governing equations are obtained as follows:

$$\phi = [A_1 e^{r1y} + A_2 e^{-r2y}]e^{i\omega t} + [A_3 e^{r3y} + A_4 e^{-r4y}]e^{-i\omega t} \quad (14)$$

$$\theta = [B_1 e^{m1y} + B_2 e^{-m2y}]e^{i\omega t} + [B_3 e^{m3y} + B_4 e^{-m4y}]e^{-i\omega t} \quad (15)$$

$$u = [C_1 e^{n1y} + C_2 e^{-n2y} + C_3 + C_4 e^{m1y} + C_5 e^{-m2y}]C_6 e^{r1y} + C_7 e^{-r2y} \times e^{i\omega t} + [D_1 e^{d1y} + D_2 e^{-d2y} + D_3 + D_4 e^{m3y} + D_5 e^{-m4y} + D_6 e^{r3y} + D_7 e^{-r4y}] \times e^{-iwt} \quad (16)$$

Using (14), (15) and (16), we write the skin friction, rate of heat transfer, and rate of mass transfer on the boundaries as follows:
The rate of skin friction or shear stress on the boundary plates is given as follows:

$$\left.\frac{du}{dy}\right|_{y=0} = [c_1 n_1 - c_2 n_2 + c_4 m_1 - c_5 m_2 + c_6 r_1 - c_7 r_2] + [D_1 d_1 - D_2 d_2 + D_4 M_3 - D_5 M_4 + D_6 r_3 - D_7 r_4]e^{-i\omega t} \quad (17)$$

$$\left.\frac{du}{dy}\right|_{y=1} = [c_1 n_1 e^{n1} - c_2 n_2 e^{-n2} + c_4 m_1 e^{m1} - c_3 m_2 e^{-m2} + c_6 r_1 e^{r1} - c_7 r_2 e^{-r2}]e^{i\omega t} + [D_1 d_1 e^{d1} - D_2 d_2 e^{-d2} + D_4 m_3 e^{m3} - D_5 m_4 e^{-m4} + D_6 r_3 e^{r3} - D_7 r_4 e^{-r4}]e^{-i\omega t} \quad (18)$$

The rate of heat transfer on the boundary plates is given as follows:

$$\left.\frac{d\theta}{dy}\right|_{y=0} = [B_1 M_1 - B_2 M_2]e^{i\omega t} + [B_3 M_3 - B_4 M_4]e^{-i\omega t} \quad (19)$$

$$\left.\frac{d\theta}{dy}\right|_{y=1} = [B_1 M_1 e^{M1} - B_2 M_2 e^{-M2}]e^{i\omega t} + [B_3 M_3 e^{M3} - B_4 M_4 e^{M4y}]e^{-i\omega t} \quad (20)$$

The rate of mass transfer on the boundary plates is given as follows:

$$\left.\frac{d\emptyset}{dy}\right|_{y=0} = [A_1 r_1 - A_2 r_2]e^{i\omega t} + [A_3 r_3 - A_4 r_4]e^{-i\omega t} \quad (21)$$

$$\left.\frac{d\emptyset}{dy}\right|_{y=1} = [A_1 r_1 e^{r1} - A_2 r_2 e^{-r2}]e^{i\omega t} + [A_3 r_3 e^{r3} - A_4 r_4 e^{r4}]e^{-i\omega t} \quad (22)$$

The constants $A_1, A_2, A_3, A_4, B_1, B_2, B_3, B_4, C_1, C_2, C_3, C_4, C_5, C_6, C_7, D_1, D_2, D_3, D_4, D_5, D_6, D_7, K_1, K_2, K_3, K_4, K_5, K_6, K_7, K_8, K_9, K_{10}, K_{11}, K_{12}, m_1, m_2, m_3, m_4, n_1, n_2, n_3, n_4, r_1, r_2, r_3 and\; r_4,$ are defined in the appendix section.

4.0 RESULTS AND DISCUSSION

Figure 4.1 is plotted to observe the influence of Grashof number and mass Grashof number. Figure 4.1a represent velocity profile for different values of Grashof number Gr (Gr = 1, 5, 10) and Figure 4.1b represent velocity profile for different values of mass Grashof number Gc (Gc = 1, 5, 10). It can be mentioned from both Figure 4.1a and 4.1b that the velocity profile increases with increasing values of Grashof number and Mass Grashof number in case of suction and Injection. It is also noticed that velocity of the fluid is higher in case of injection than suction. What causes

DOI: https://doi.org/10.57233/ijsgs.v10i1.600 ISSNp: 2488-9229; ISSNe: 3027-1118

IJSGS FUGUSAU VOL. 10(1) WEBSITE: https://fugus-ijsgs.com.ng

this behavior is that, in case of suction, the fluid at ambient conditions is brought closer to the surface and reduces the thermal boundary layer thickness. The same principle operates but in reverse direction in case of injection. The velocity profiles for different values of Jeffrey fluid parameter (β_1=0.1, 0.2, 0.3) and Hartmann number (H = 1, 2, 3)are shown in Figures 4.2a and 4.2b respectively. It is observed that the velocity increase with increasing values of Jeffrey fluid parameter in case of suction and Injection but decreases with increasing Hartmann number for suction and Injection. As Jeffrey fluid parameter is increases, the fluid becomes more resistant to flow and its velocity profile becomes more uniform and less prone to distortion compared to a less elastic fluid.

Figure 4.3a and 4.3b represent the influence of heat source/sink parameter (Q=1, 5, 10) on velocity and temperature profiles respectively in case of suction and injection. Both velocity and temperature of the fluid increases with increasing values of heat source (Q>0) while a reverse trend is observed in case of heat sink (Q<0). The presence of heat source indicates higher temperature generation while heat sink indicates heat absorption in the channel. In Figure 4.4a and 4.4b, the velocity and temperature profiles for different values of Peclet number (Pe = 1, 2, 3, 4) is presented respectively in case of suction and injection of the fluid. Increasing values of Peclet number enhances both velocity and temperature profiles in case of suction and injection of the fluid. It is seen that both temperature and velocity profiles are higher in case of injection than suction. Figure 4.5a and 4.5b are plotted to see the impacts of Radiation parameter (N = 1, 2, 2.5) on both velocity and temperature distribution respectively in case of sucking and injecting fluid into the channel walls. Higher values of Radiation parameter improved fluid velocity and temperature in case of suction and injection of the fluid.

The velocity and concentration profiles have been presented in Figures 4.6a and 4.6b respectively for different values of the mass transfer Peclet number (Pem = 1, 2, 3, 4) in case of suction and injection. It is observed that both the velocity and the concentration increase with increasing values of Peclet number. An anomalous behavior is noticed on the velocity profile in case of suction, velocity is higher than in case of injection at around center of the channel. What cause this behavior is the oscillating nature of the fluid.

The variation of the skin friction ($\tau_0 and \tau_1$) on the porous plate with material parameters are shown in figures 4.7 to figure 4.12. The skin friction ($\tau_0 and \tau_1$) profiles for different values of heat source/sink parameter (Q=1, 5, 10) are shown in Figure 4.7. It is observed that skin friction at y = 0 (τ_0) increases with increasing values of heat source (Q>0) while opposite phenomenon is noticed for increasing values of heat sink (Q<0).At the plate y = 1 opposite trend is observed. The skin friction against Reynold number (Re) for different values of Radiation parameter (N = 1, 2, 2.5) are shown in Figure 4.8. Figure 4.8a represent skin friction at the plate y = 0 and Figure 4.8b represent skin friction at the plate y = 1 respectively. From Figure 4.8a it is seen skin friction is enhanced by increasing values of Radiation parameter in case of suction and injection. It is observed that skin friction is higher in case of injection than suction. Similar scenario is noticed but in opposite direction in Figure 4.8b. The shear stress against Reynold number for different values of Hartmann number (H = 1, 2, 3) at the plate y = 0 and y = 1 are shown in Figure 4.9a an 4.9b respectively. It is observed that skin friction, skin friction decreases with increasing values of Hartman number at the plate y = 0 but opposite trend is noticed at plate y = 1.

The skin friction at y = 0 and y = 1 for different values of Grashof number Gr (Gr = 1, 5, 10) are shown in Figure 4.10a and 4.10b respectively in case of suction and injection. It is observed that skin friction at y = 0 and y =1 increases with increasing values of Grashof number in case of suction and injection. It is also noticed that at plate y = 0 skin friction is higher in case of suction then injection but opposite trend is observed at the plate y = 1. The skin friction against t for different values of Mass Grashof number Gc (Gc = 1, 5, 10) are shown in Figure 4.11a and 4.11b respectively at the plate y = 0 and y = 1. Similar behavior is noticed for the case of Grashof number in Figure 4.2.10. The skin friction ($\tau_0 and \tau_1$) profiles for different values of Jeffrey fluid parameter (β_1=0.1, 0.2, 0.3) are shown in figure 4.12. It is observed that skin friction (τ_0) increase with increasing Jeffrey fluid parameter but skin friction (τ_1) decrease with increasing Jeffrey fluid parameter.

The variation of the Nusselt number against t for different values of heat source/sink parameters shown in Figure 4.13a and 4.13b respectively at the plate y = 0 and y = 1. Increasing values of heat source parameter enhances Nusselt number while increasing heat sink parameter decreases Nusselt number at the plate y = 0 but opposite behavior is seen at the plate y = 1. The Nusselt number ($Nu_0 \; and \; Nu_1$) profiles for different values of Radiation parameter (N = 1, 1.5, 2, 2.5) is shown in Figure 4.14a and 4.14b at the plate y = 0 and y =1 respectively. It observed that Nusselt number (Nu_0) increases with increasing Radiation parameter while the Nusselt number(Nu_1)decreases with increasing Radiation parameter.

The variation of the Sherwood number against suction/injection parameter for different values of mass Peclet number (Pm = 1, 2, 3, 4) is shown in Figure 15a and 15b respectively at y = 0 and y = 1. Higher values of Sherwood number is recorded when the

DOI: https://doi.org/10.57233/ijsgs.v10i1.600 ISSNp: 2488-9229; ISSNe: 3027-1118

IJSGS FUGUSAU VOL. 10(1) WEBSITE: https://fugus-ijsgs.com.ng

suction/injection parameter values is large at the plate y = 0 (Fig.15a), however similar trend is observed at y = 1 (Fig.15b).

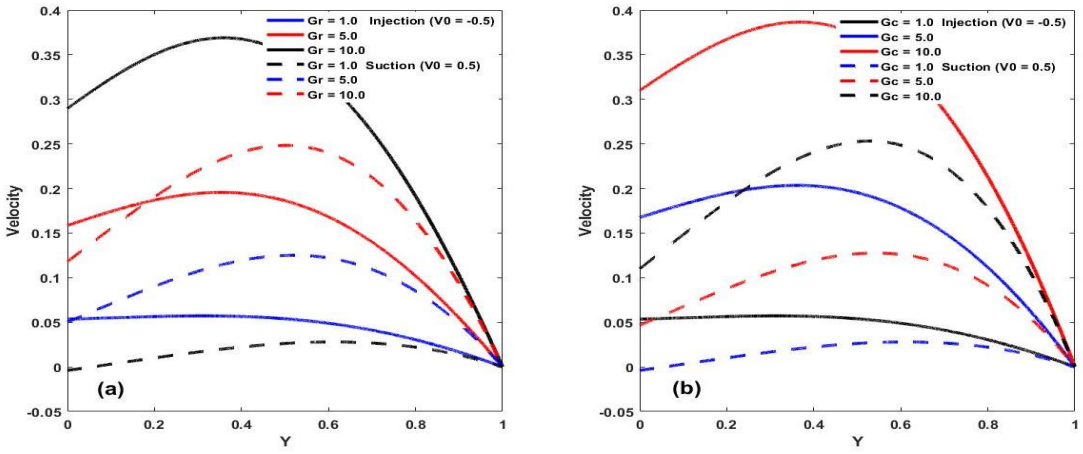

Figure 1 (a and b): Velocity profiles for different values of Gr and Gc

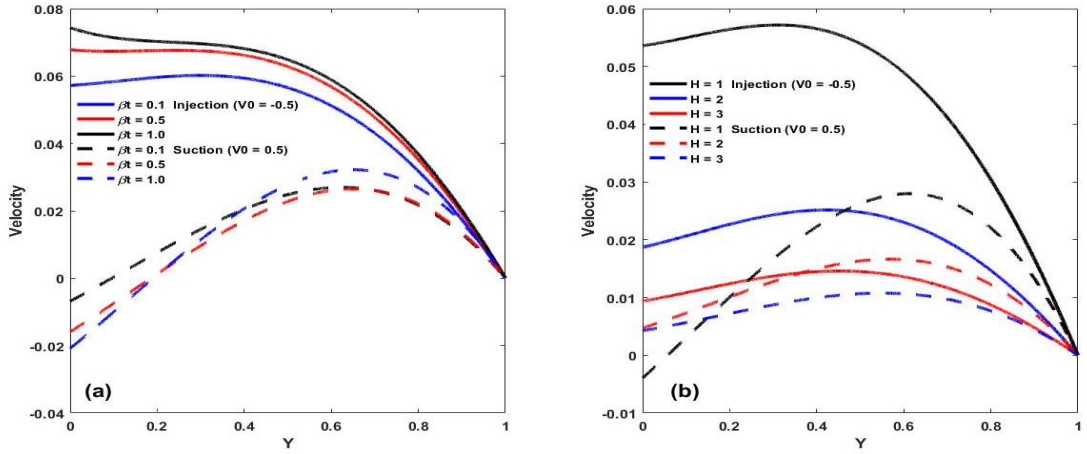

Figure 2 (a and b): Velocity profiles for different values of β_1 and H

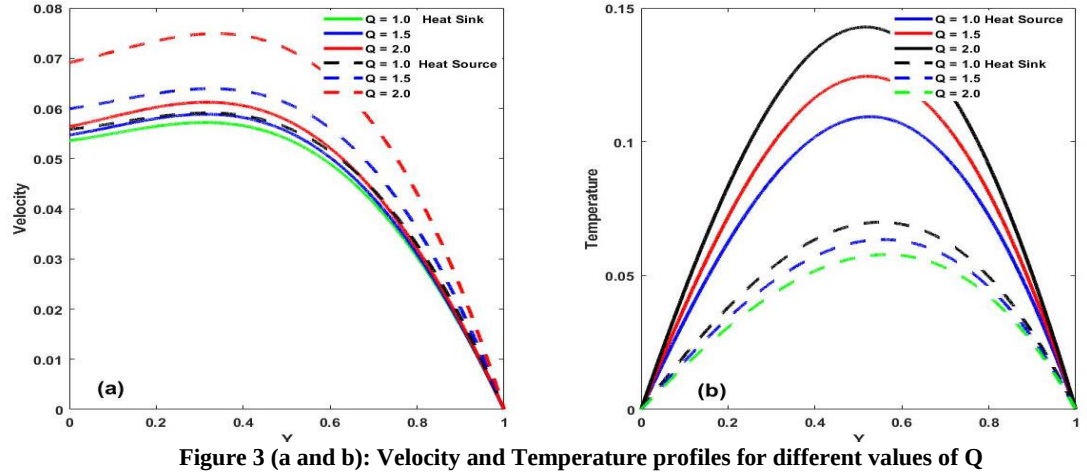

Figure 3 (a and b): Velocity and Temperature profiles for different values of Q

DOI: https://doi.org/10.57233/ijsgs.v10i1.600 ISSNp: 2488-9229; ISSNe: 3027-1118

IJSGS FUGUSAU VOL. 10(1) WEBSITE: https://fugus-ijsgs.com.ng

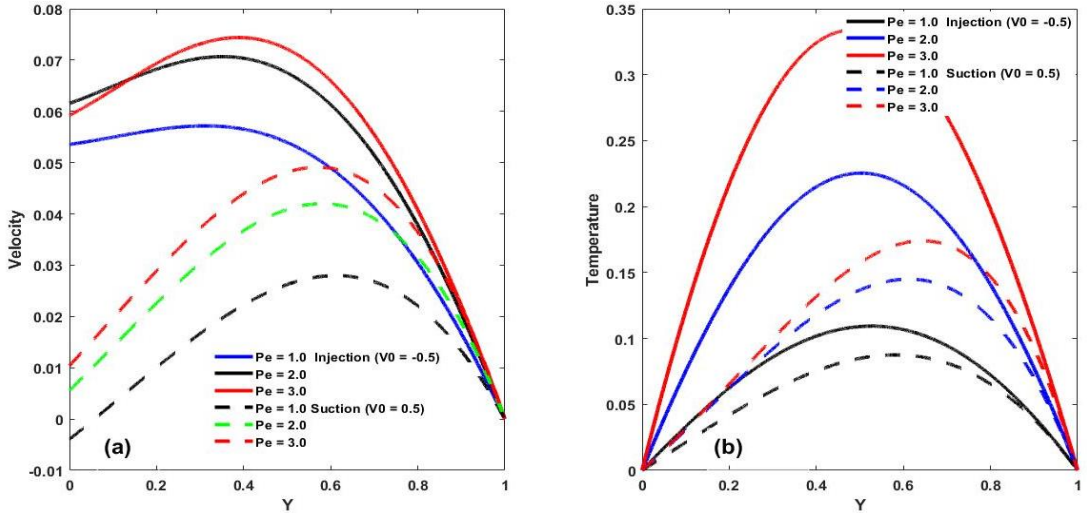

Figure 4 (a and b): Velocity and temperature profiles for different values of Pe

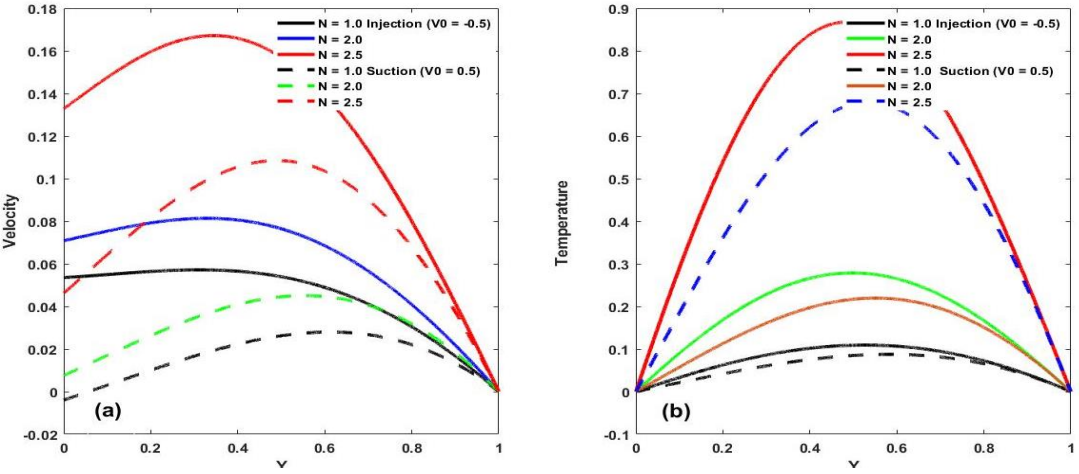

Figure 5 (a and b): Velocity and temperature profiles for different values of N

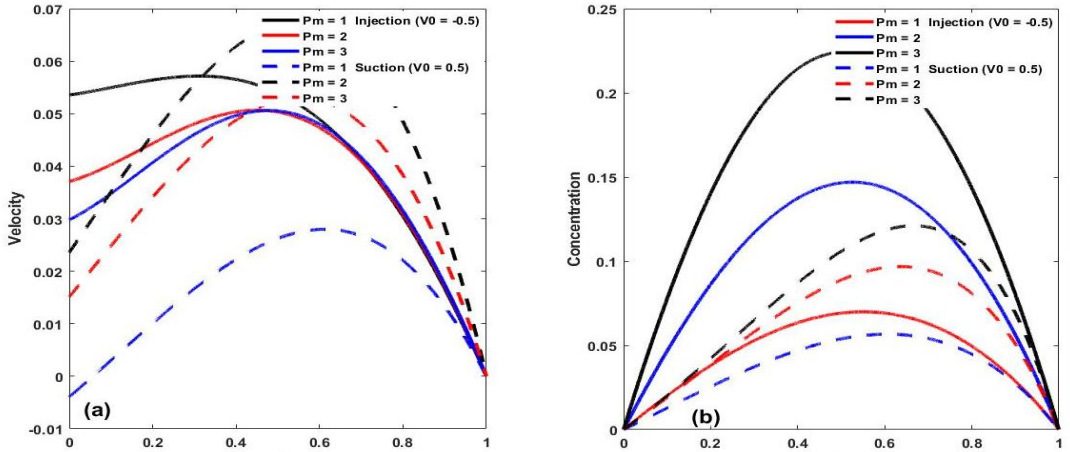

Figure 6 (a and b): Velocity and concentration profiles for different values of Pm

DOI: https://doi.org/10.57233/ijsgs.v10i1.600 ISSNp: 2488-9229; ISSNe: 3027-1118

IJSGS FUGUSAU VOL. 10(1) WEBSITE: https://fugus-ijsgs.com.ng

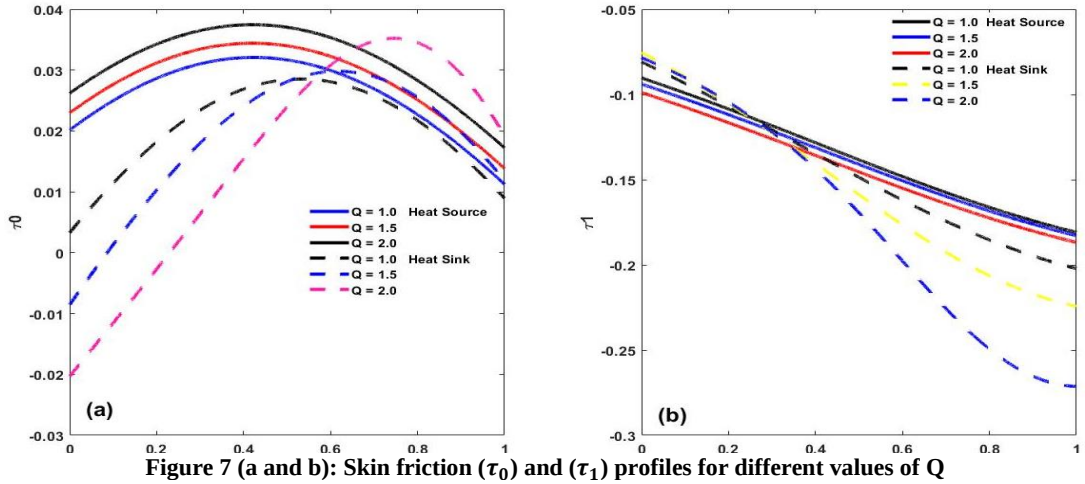

Figure 7 (a and b): Skin friction (τ_0) and (τ_1) profiles for different values of Q

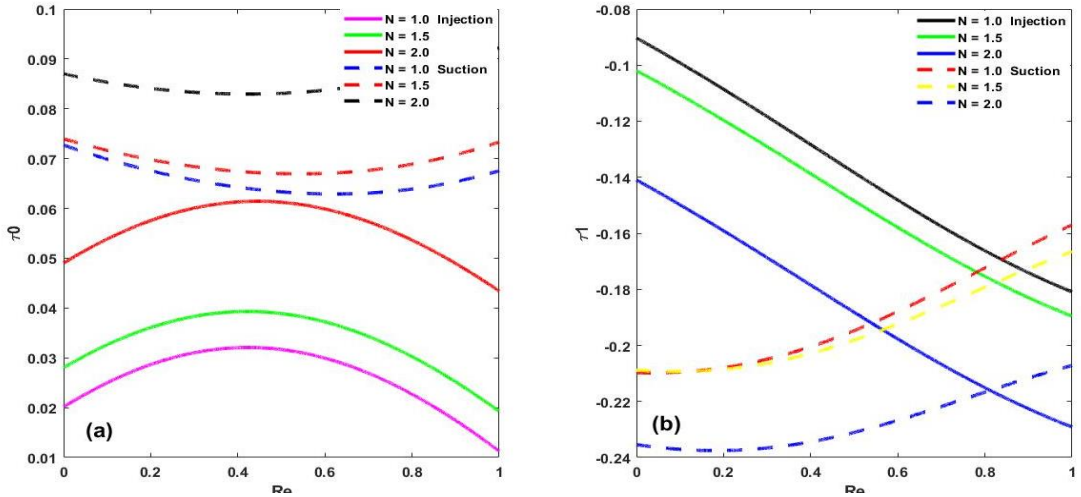

Figure 8 (a and b): Skin friction (τ_0) and (τ_1) profiles for different values of N

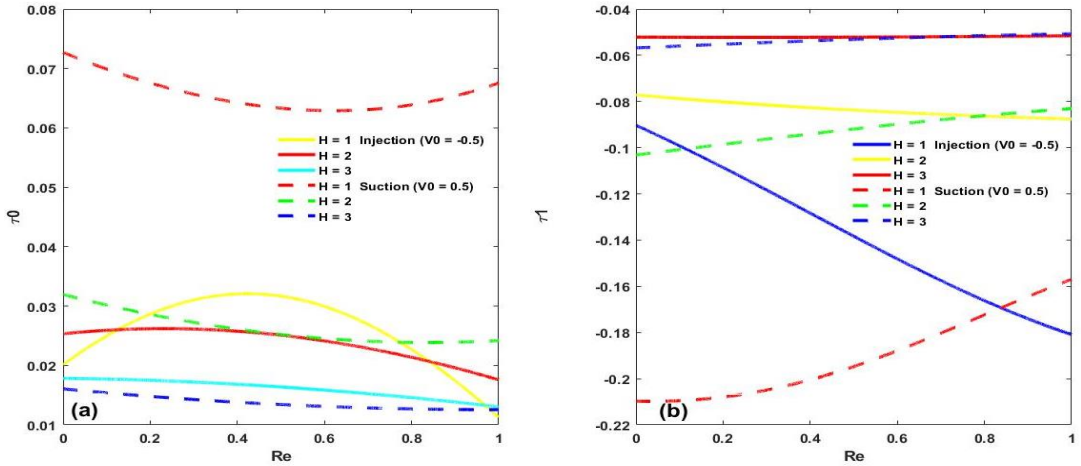

Figure 9 (a and b): Skin friction (τ_0) and (τ_1) profiles for different values of H

DOI: https://doi.org/10.57233/ijsgs.v10i1.600 ISSNp: 2488-9229; ISSNe: 3027-1118

IJSGS FUGUSAU VOL. 10(1) WEBSITE: https://fugus-ijsgs.com.ng

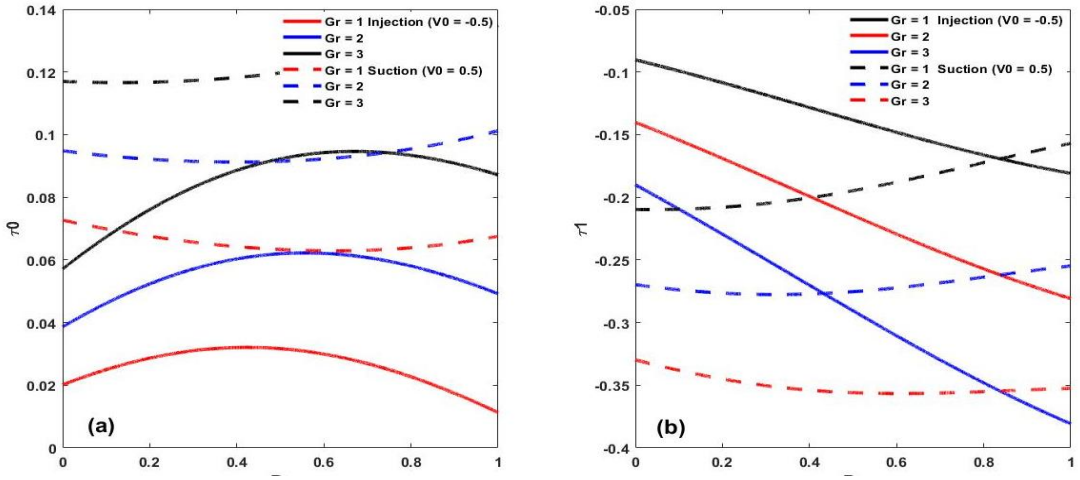

Figure 10 (a and b): Skin friction (τ_0) and (τ_1) profiles for different values of Gr

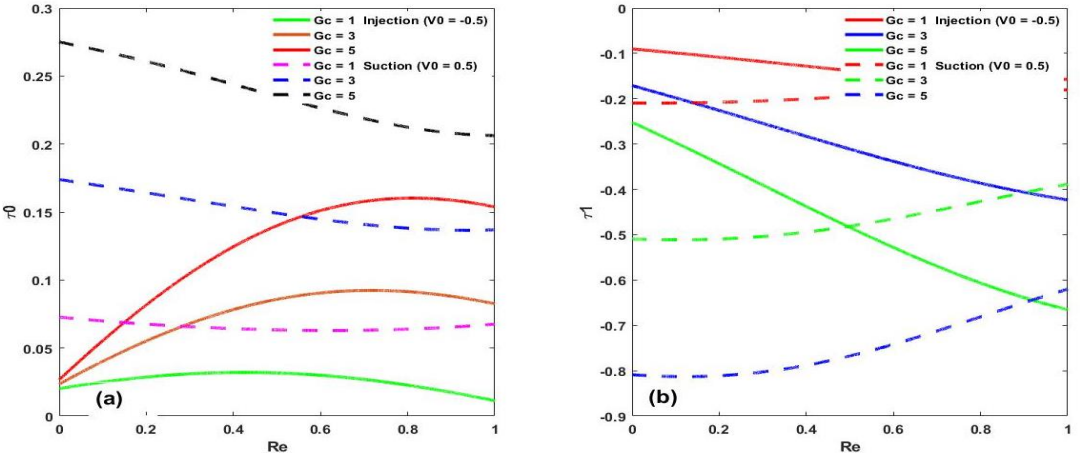

Figure 11 (a and b): Skin friction (τ_0) and (τ_1) profiles for different values of Gc

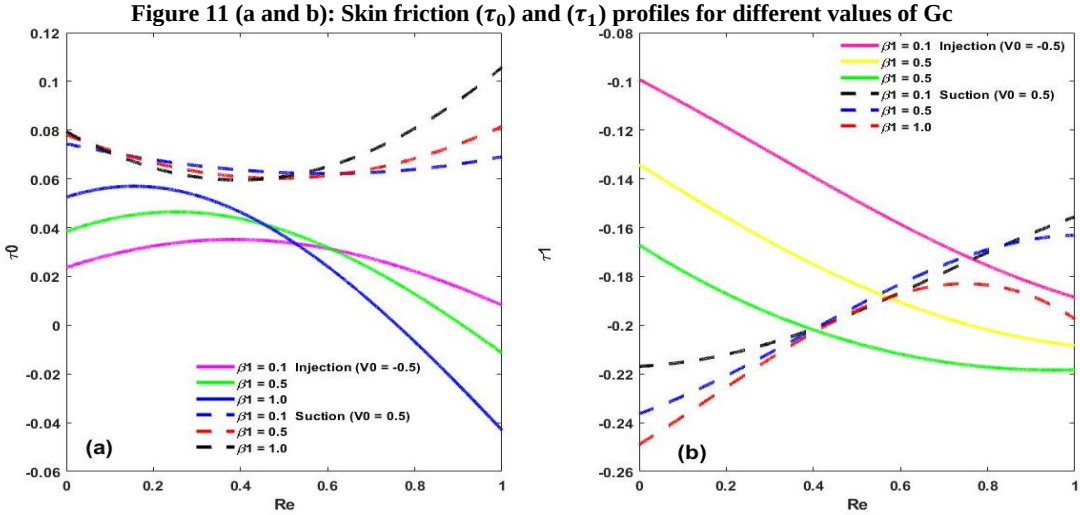

Figure 12 (a and b): Skin friction (τ_0) and (τ_1) profiles for different values of β_1

DOI: https://doi.org/10.57233/ijsgs.v10i1.600 ISSNp: 2488-9229; ISSNe: 3027-1118
IJSGS FUGUSAU VOL. 10(1) WEBSITE: https://fugus-ijsgs.com.ng

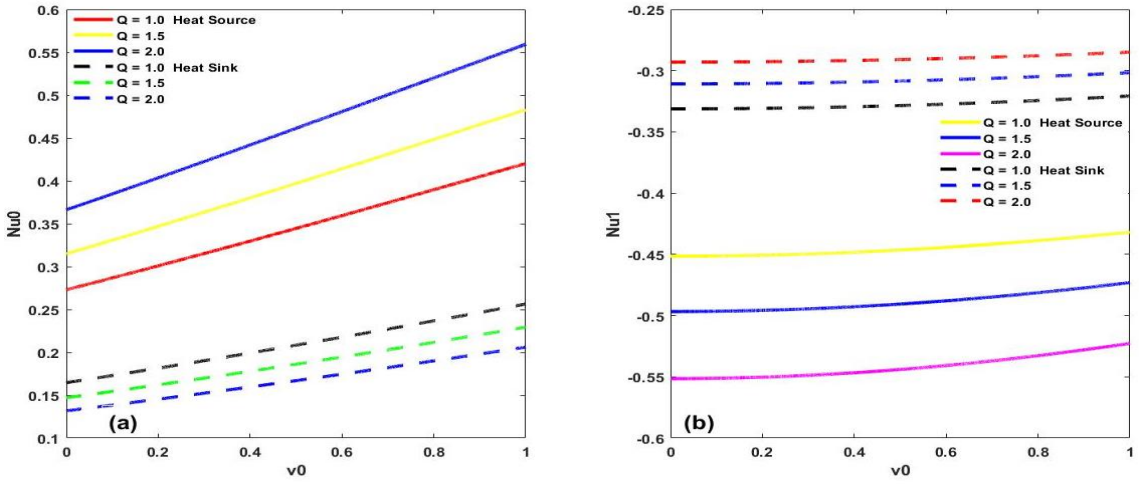

Figure 13 (a and b): Nusselt number (Nu0) and (Nu1) profiles for different values of Q

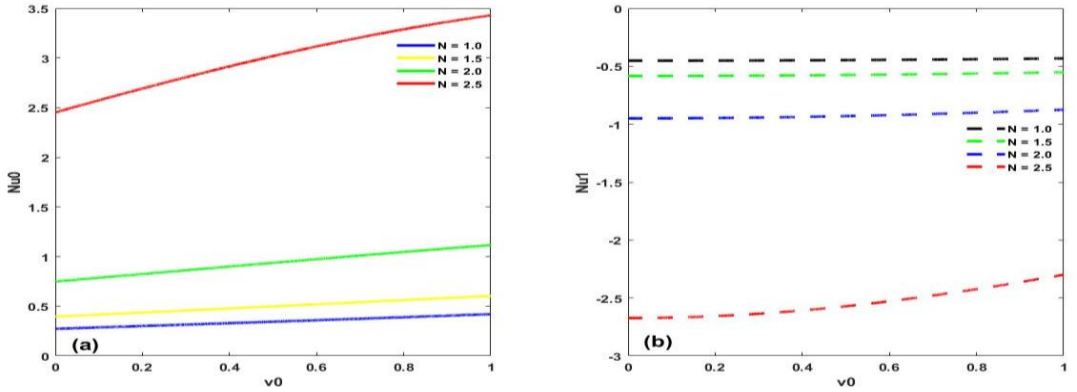

Figure 14 (a and b): Nusselt number (Nu0) and (Nu1) profiles for different values of N

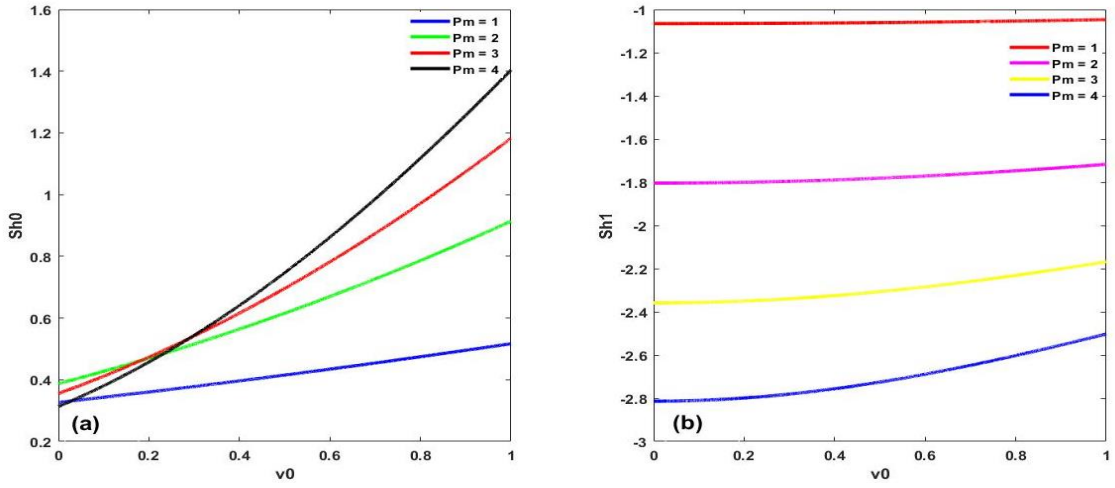

Figure 15 (a and b): Sherwood number (Sh0 and Sh1) profiles for different values of Pm

5.0 CONCLUSION

In this present study, an analytical investigation has been carried out to study unsteady MHD free convective flow of Jeffrey fluid through porous medium with effect of heat source/sink. Solutions for the model have been obtained by using regular perturbation techniques. The following conclusions are made:

i. It is observed that the velocity of the fluid increases with increasing values of Grashof number and Mass Grashof number in case of suction and Injection. It is noticed that velocity of the fluid is higher in case of injection than suction.
ii. It is noticed that the velocity increase with increasing values of Jeffrey fluid parameter in case of suction and Injection but decreases with increasing Hartmann number for suction and Injection.
iii. Both velocity and temperature of the fluid increases with increasing values of heat source

(Q>0) while a reverse trend is observed in case of heat sink (Q<0).

iv. Increasing values of Peclet number enhances both velocity and temperature profiles in case of suction and injection of the fluid. It is seen that both temperature and velocity profiles are higher in case of injection than suction.

v. Higher values of Radiation parameter improved fluid velocity and temperature in case of suction and injection of the fluid.

vi. It is observed that both the velocity and the concentration increase with increasing values of Peclet number. An anomalous behavior is noticed on the velocity profile in case of suction, velocity is higher than in case of injection at around center of the channel.

vii. It is observed that the skin-friction coefficient at the plate (when y = 0) increases with increasing values of heat source (Q>0) while opposite phenomenon is noticed for increasing values of heat sink (Q<0) at the plate (when y = 1) opposite trend is observed.

viii. It is seen that skin friction is enhanced by increasing values of Radiation parameter in case of suction and injection (when y = 0). It is observed that skin friction is higher in case of injection than suction. Similar scenario is noticed but in opposite direction (when y = 1)

ix. It is observed that skin friction, the skin-friction coefficient decreases with increasing values of Hartman number at the plate (when y = 0) but opposite trend is noticed at plate (when y = 1).

x. It is observed that skin friction (when y = 0) increase with increasing Jeffrey fluid parameter but skin friction (when y = 1) decrease with increasing Jeffrey fluid parameter.

xi. Increasing values of heat source parameter enhances the rate of heat transfer while increasing heat sink parameter decreases the rate of heat transfer at the plate (when y = 0) but opposite behavior is seen at the plate (when y = 1).

xii. It observed that the rate of heat transfer (when y = 0) increases with increasing Radiation parameter while (when y = 1) decreases with increasing Radiation parameter.

REFERENCES

Bafakeeh O. T., Raza A., Khan U. S., Khan M. I., Nasr A., Khedher N.B. and Tag-Eldin E.M. (2022). Physical interpretation of Nanofluid (Copper Oxide and Silver) with slip and mixed convection effects: Application of fractional derivatives; *Applied Sciences*, 12 (21), 10.3390/app122110860.

Chitra M. and Suhasini M. (2018). Effect of unsteady oscillatory MHD flow through a porous medium in porous vertical channel with chemical reaction and concentration, National Conference on Mathematical Techniques and its Applications, 012039, doi :10.1088/1742-6596/1000/1/012039

Chu Y., Aziz S., Ijaz K. M., Khan S. U., Nazeer M., Ahmad I. and Tlili, I. (2020). Nonlinear radiative bioconvection flow of Maxwell nanofluid configured by bidirectional oscillatory moving surface with heat generation phenomenon, Physica Scriptavol 95(10). https://doi.org/10.1088/1402-4896/abb7a9

Cioranescu, D., Girault, V. and Rajagopal, K. R. (2016). Mechanics and Mathematics of Fluids of the Differential Type, Advances in Mechanics and Mathematics, 35 (1)

Falade, J. A., Ukaegbu, J., Egere, A. C., and Adesanya, S., (2017). MHD Oscillatory Flow Through a Porous Channel Saturated with Porous Medium, Alexandria Eng. J., 56(1), pp. 147–152. Doi:10.1016/j.aej.2016.09.016

Gambo D., Yusuf, T. S., Oluwagbemiga, S. A., Kozah, J. D. and Gambo J. J. (2021). Analysis of free convective hydromagnetic flow of heat generating/absorbing fluid in an annulus with isothermal and adiabatic boundaries. Partial Differential Equations in Applied Mathematics. https://doi.org/10.1016/j.padiff.2021.100080

Gambo J. and Gambo D. (2020). On the effect of heat generation/absorption on magneto-hydrodynamic free convective flow in a vertical annulus: An Adomian decomposition method. Heat transfer, Wiley. 50(1), 1-15. DOI: 10.1002/hti.21978.

Hamza, M. M. Usman, H. Mustafa A. and Isah B. Y. (2011). Chemical Reaction and Slip Condition Effects on MHD Oscillatory Flow Through a Porous Medium, Research Journal of Mathematic and Statistics, 3(4), pp. 130-135.

Hartmann, J. and Lazarus, F. (1937). Hg-dynamics II: theory of laminar flow of electrically conductive liquids in a homogeneous magnetic field, Matematisk-Fysiske Meddelelser, 15(7).

Hasan, N. Z. Mohammed, Y. Nasreen, S. N. (2020). Effects of thermal radiation, heat generation and induced Magnetic field on Hydromagnetic free convective flow of couple stress fliud in an isoflux-isothermal vertical channel, Journal of Applied Mathematics, vol.2020, Article ID 4539531.

Ibrahim, M. Yale, I. D. Hamza, M.M. F. Abubakar (2020). The effect of suction/injection on MHD oscillatory flow of Jeffrey fluid with heat source/sink through a porous medium, Int. J. Adv. Eng. and Mangt. 2(8), pp 268-274.

Jawad, M., Saeed, A. and Gul, T. (2021). Entropy generation for MHD Maxwell nanofluid flow past a porous and stretching surface with Dufour and Soret

effects. Brazilian. Journal of Physics, pp. 1-13. Doi: 10.1007/s1353802000835-x

Kahshan, M., Lu, D. and Siddiqui, A. M. (2019). A Jeffrey Fluid Model for a Porous-walled Channel: Application to Flat Plate Dialyzer, Scientific Reports, 9. pp. 15-25. Doi.org/10.1038/s41598019-52346-8

Khan, A., Zaman, G. and Algahtani, O. (2018). Unsteady Magnetohydrodynamic Flow of Jeffrey Fluid through a Porous Oscillating Rectangular Duct. Porosity Process, Technological Applications, pp. 125–128. Doi: 10.5772/intechopen.70891

Magnon, E. and Cayeux, E. (2021). Precise Method to Estimate the Herschel-Bulkley Parameters from Pipe Rheometer Measurements. Fluids, 6, 157. Doi:10.3390/fluids6040157

Nadeem, S., Akhtar, S. and Saleem, A. (2021). Peristaltic flow of a heated Jeffrey fluid inside an elliptic duct: Streamline analysis. Applications in Mathematics and Mechanics, 42, pp. 583–592. Doi.org/10.1007/s10483-02127146

Narayana P.V. S. and Venkateswarlu B. (2016). Heat and mass transfer on mhd nanofluid flow past a vertical porous plate in a rotating system, Frontiers in Heat and Mass Transfer, 7(8), DOI: 10.5098/hmt.7.8

Ojemeri G. and Onwubuya I. O. (2023). Analysis of mixed convection flow on Arrhenius-controlled heat generating/absorbing fluid in a superhydrophobic microchannel: A semi-analytical approach, Dutse Journal of Pure and Applied Sciences, 9, 344-357. DOI:104314/dujopas.v9i2a.34

Ojemeri, G. and Hamza, M. M. (2022). Heat transfer analysis of Arrhenius-controlled free convective hydromagnetic flow with heat generation/absorption effect in a micro-channel, Alexandria Engineering Journal, 61, pp. 12797-12811. DOI: 10.1016j.aej.2022.06.58

Ojemeri, G., Onwubuya I. O., Omokhuale, E., Hussaini A. and Shuaibu, A. (2024). Analytical investigation of Arrhenius kinetics with heat source/sink impacts along a heated superhydrophobic microchannel, UMYU Scientifica, 3(1), 61-71. DOI:105619/usci.2431.004

Oni M. O. and Jha B. K. (2019). Heat generation/absorption effect on natural convection flow in a vertical annulus with time-periodic boundary conditions. Journal of Aircraft and Spacecraft technology, 3(1), 183-196. https://doi.org/10.3844/jastsp.2019.183.196

Parthiban S. and Prasad V. R. (2023). Thermal radiation and Hall current effects in a MHD non-Darcy flow in a differentially heated square enclosure Lattice-Boltzmann simulation. Journal of porous media, Begell house, 26(5), pp37-56. DOI: 10.1615/JPorMedia.2022044054.

Sajid, M., Jagwal, M. R. and Ahmad, I. (2021). Numerical and perturbative analysis on non-axisymmetric Homann stagnation-point flow of Maxwell fluid. SN Applied Sciences,3, 438. Doi.org/10.1007/s42452-021-04344-7

Sharma T., Sharma P. and Kumar N. (2022). Study of dissipative MHD oscillatory unsteady free convective flow in a vertical channel occupied with the porous material in the presence of heat source effect and thermal radiation, International Symposium on Fluids and Thermal Engineering, 012012. doi:10.1088/1742-6596/2178/1/012012.

Sharma, B. D., Yadav, P. K. and Filippov, A. (2017). A Jeffrey-fluid model of blood flow in tubes with stenosis, Colloid Journal, 79, pp. 849–856. Doi.org/10.1134/S1061933X1706014X

Suma U. K., Katun M. and Biswas R. (2023). Consequences of Thermophoresis, and Brownian Motion on MHD Heat and Mass Transfer of Jeffrey's Nano-fluid Flow Via a Perpendicular Plate, Asian Journal of Pure and Applied Mathematics, 5(1), 414-429, https://gloalpresshu.com.idex,php/AJPAM/article/view/1880

Usman H. and Sanusi S. (2023). Heat and mass transfer analysis for the mhd flow of Casson nanofluid in the presence of thermal radiation, FUDMA Journal of Sciences, 7(2), pp 188 – 198. https:doi.org/10.33003/fjs-2023-0702-1728

Vaidya, H., Rajashekhar, C., Divya, B.B., Manjunatha, G., Prasad, K. V. and Animasaun, I. L. (2020). Influence of transport properties on the peristaltic MHD Jeffrey fluid flow through a porous asymmetric tapered channel, Results in Physics, 18, DOI:101016/j.rinp.2020.103295.

Wang, J., Khan, M. I., Khan, W. A., Abbas, S. Z. and Khan, M. I. (2019). Transportation of heat generation/absorption and radiative heat flux in homogeneous-heterogeneous catalytic reactions of non-Newtonian fluid (Oldroyd-B model), Computational Methods in Programs and Biomedicals, doi:105310.1016/j.cmpb.2019.105310

Yale, I. D, Aisha, A. H., Mustapha, I. and Muhammad, M. H. (2019). Unsteady Heat Transfer to MHD Oscillatory flow of Jeffrey fluid in Channel filled with porous material. International Journal of Scientific and Research Publications, 9(7), http://dx.doi.org/10.29322/IJSRP.9.07.2019.P178.

Zhao T., Khan M. and Chu Y. (2020) Artificial neural networking (ANN) analysis for heat and entropy generation in flow of non-Newtonian fluid between two rotating disks, Math. Method Applied Sci, https://doi.org/10.1002/mma.7310

DOI: https://doi.org/10.57233/ijsgs.v10i1.600 **ISSNp:** 2488-9229; **ISSNe:** 3027-1118

IJSGS FUGUSAU VOL. 10(1) **WEBSITE: https://fugus-ijsgs.com.ng**

Appendix

$$A_1 = \frac{-1}{2[e^{-r_2} - e^{r_1}]},\quad A_2 = \frac{1}{2[e^{-r_2} - e^{r_1}]},\quad A_3 = \frac{-1}{2[e^{-r_4} - e^{r_3}]},\ A_4 = \frac{1}{2[e^{-r_4} - e^{r_3}]}$$

$$B_1 = \frac{-1}{2[e^{-M2} - e^{M1}]}, B_2 = \frac{1}{2[e^{-M2} - e^{M1}]},\quad B_3 = \frac{-1}{2[e^{-M4} - e^{M3}]}, B_4 = \frac{1}{2[e^{-M_4} - e^{M_3}]}$$

$$C_1 = \frac{rk_3k_6 - k_2k_6 - k_5k_7}{k_4k_6}, C_2 = \frac{k_7}{k_6}, C_3 = \frac{\succ K_1}{\propto_2}, C_4 = \frac{-GrK_1B_1}{{M_1}^2 + \propto_1 M_1 - \propto_2},$$

$$C_5 = \frac{-GrK_1B_2}{{M_2}^2 + \propto_1 M_2 - \propto_2}, C_6 = \frac{-GcK_1A_1}{{r_1}^2 + \propto_1 r_1 - \propto_2}, C_7 = \frac{-GcK_1A_2}{{r_2}^2 - \propto_1 r_2 - \propto_2}$$

$$D_1 = \frac{rk_9k_{13} - k_8k_{13} - k_{11}k_{14}}{k_{10}k_{13}}, D_2 = \frac{K_{14}}{K_{13}}, D_3 = -\frac{\succ K_1}{\propto_3}, D_4 = \frac{-hrK_1B_3}{{M_3}^2 + \propto_1 M_3 - \propto_3}$$

$$D_5 = \frac{-GrK_1B_4}{{M_4}^2 - \propto_1 M_4 + \propto_3}, D_6 = \frac{-GcK_1A_3}{{r_3}^2 + \propto_1 r_3 + \propto_3}, D_7 = \frac{-hcK_1A_4}{{r_4}^2 - \propto_1 r_4 + \propto_3}$$

$$K_1 = 1 + \beta_t,\ K_2 = C_3 + C_4 + C_5 + C_6 + C_7,\ K_3 = C_4n_1 - C_5n_2 + C_6m_1 - C_7m_2$$

$$K_4 = 1 - r_{r_1}, K_5 = 1 + r_{r_2},\ K_6 = k_4e^{-r2} - k_5e^{r1},$$

$$K_7 = -rk_3e^{r1} - C_3k_4 - C_4k_4e^{n1} - C_5k_4e^{-n2} - C_6k_4e^{m1} - C_7k_4e^{-m2}$$

$$K_8 = D_3 + D_4 + D_5 + D_6 + D_7,\qquad K_9 = D_4n_3 - D_5n_4 + D_6m_1 - D_7m_4$$

$$K_{10} = 1 - r_{r_3}, K_{11} = 1 + r_{r_4}\ K_{12} = rk_9 - k_8$$

$$m_1 = \frac{-V_oP_m + \sqrt{{V_0}^2{P_m}^2 + 4a_1}}{2}, m_2 = \frac{V_oP_m + \sqrt{{V_0}^2{P_m}^2 + 4a_1}}{2},$$

$$m_3 = \frac{-V_oP_m + \sqrt{{V_0}^2{P_m}^2 - 4a_2}}{2}, m_4 = \frac{V_oP_m + \sqrt{{V_0}^2{P_m}^2 - 4a_2}}{2}$$

$$n_1 = \frac{-V_oP_e + \sqrt{{V_0}^2{P_e}^2 - 4(b - iP_ew)}}{2}, n_2 = \frac{V_oP_e + \sqrt{{V_0}^2{P_e}^2 - 4(b - iP_ew)}}{2},$$

$$n_3 = \frac{-V_oP_e + \sqrt{{V_0}^2{P_e}^2 - 4(b + iP_e\omega)}}{2},\ n_4 = \frac{V_oP_e + \sqrt{{V_0}^2{P_e}^2 - 4(b + iP_e\omega)}}{2}$$

$$r_1 = \frac{-\propto_1 + \sqrt{{\propto_1}^2 - 4\propto_2}}{2},\ r_2 = \frac{\propto_1 + \sqrt{{\propto_1}^2 - 4\propto_2}}{2}, r_3 = \frac{-\propto_1 + \sqrt{{\propto_1}^2 - 4\propto_3}}{2}$$

$$r_4 = \frac{\propto_1 + \sqrt{{\propto_1}^2 - 4\propto_3}}{2}$$